JOURNAL OF VIROLOGY, May 2010, p. 4556–4568 Vol. 84, No. 9
0022-538X/10/$12.00 doi:10.1128/JVI.02545-09

T Cells Facilitate Recovery from Venezuelan Equine Encephalitis Virus-Induced Encephalomyelitis in the Absence of Antibody▽

Christopher B. Brooke,[1,2]* Damon J. Deming,[1,2] Alan C. Whitmore,[2] Laura J. White,[1,2] and Robert E. Johnston[1,2]

Department of Microbiology & Immunology,[1] Carolina Vaccine Institute,[2] University of North Carolina at Chapel Hill, Chapel Hill, North Carolina 27599

Received 4 December 2009/Accepted 9 February 2010

Venezuelan equine encephalitis virus (VEEV) is a mosquito-borne RNA virus of the genus *Alphavirus* that is responsible for a significant disease burden in Central and South America through sporadic outbreaks into human and equid populations. For humans, 2 to 4% of cases are associated with encephalitis, and there is an overall case mortality rate of approximately 1%. In mice, replication of the virus within neurons of the central nervous system (CNS) leads to paralyzing, invariably lethal encephalomyelitis. However, mice infected with certain attenuated mutants of the virus are able to control the infection within the CNS and recover. To better define what role T cell responses might be playing in this process, we infected B cell-deficient μMT mice with a VEEV mutant that induces mild, sublethal illness in immune competent mice. Infected μMT mice rapidly developed the clinical signs of severe paralyzing encephalomyelitis but were eventually able to control the infection and recover fully from clinical illness. Recovery in this system was T cell dependent and associated with a dramatic reduction in viral titers within the CNS, followed by viral persistence in the brain. Further comparison of the relative roles of T cell subpopulations within this system revealed that $CD4^+$ T cells were better producers of gamma interferon (IFN-γ) than $CD8^+$ T cells and were more effective at controlling VEEV within the CNS. Overall, these results suggest that T cells, especially $CD4^+$ T cells, can successfully control VEEV infection within the CNS and facilitate recovery from a severe viral encephalomyelitis.

Venezuelan equine encephalitis virus (VEEV) is a mosquito-borne RNA virus of the genus *Alphavirus* that is responsible for a significant disease burden in Central and South America through sporadic outbreaks into human and equid populations (20, 57). The most recent major outbreak occurred in 1995 with 75,000 to 100,000 human cases spread between Columbia and Venezuela (59). For humans, only 1 to 2% of cases progress to full-blown encephalitis, though roughly 50% of those cases are fatal (58). In equid populations, however, the mortality rate is much higher and is often over 50% (56). Because of the high probability of future natural outbreaks, as well as its potential use as a bioterrorism agent, VEEV remains a significant public health concern (43). Currently, there are no therapeutics or licensed vaccines available for human use.

Work with multiple infection models has shown that both the innate and adaptive arms of the host immune response are involved in successful control of viruses that target central nerve system (CNS) neurons (21). Disruption of the type I interferon system dramatically decreases the average survival time of mice infected with VEEV, as well as of those infected with Sindbis and West Nile viruses (45, 46, 60). Studies performed with a variety of neuronotropic viruses, including Sindbis and West Nile viruses, have clearly demonstrated that the development of a virus-specific antibody response is a critical step in both limiting viral spread and facilitating noncytolytic clearance of infectious virus from neurons within the brain (14, 32). α/β T cell responses also help limit lethality in many of these models by directly killing infected cells, producing antiviral cytokines, and/or enhancing the production and quality of virus-specific antibody (4, 38, 52, 54). In the case of Sindbis virus, the T cell compartment was able to dramatically restrict viral replication in the CNS in the absence of antiviral antibodies, partly through a gamma interferon (IFN-γ)-dependent mechanism (5). While numerous components of the host immune system play a role in mediating protection or recovery from neuronotropic virus infection, the specific mechanisms by which the host is able to eliminate virus from CNS neurons, while leaving these critical, irreplaceable cells intact, remain unknown.

Our current understanding of VEEV pathogenesis comes primarily from work performed using a well-established mouse model of infection and disease that closely mirrors many aspects of disease in humans and horses (18). Following peripheral inoculation into the footpad of a mouse, a delivery method that mimics the natural route of infection by mosquito bite, the virus initiates a biphasic course of infection in which initial replication within the skin-draining lymph node as well as other secondary lymphoid tissue seeds a high-titer serum viremia (35). The viremia facilitates virus invasion of the CNS, initially through nonmyelinated olfactory neurons within the nasal neuroepithelium (11, 35). This leads to a second phase of infection characterized by rapid replication and spread though CNS neurons and the eventual development of paralyzing encephalitis (10, 19). Infection of inbred mice with most strains of VEEV results in 100% mortality (56). Due to the extreme lethality of the virus, efforts to understand the host mecha-

* Corresponding author. Mailing address: The Carolina Vaccine Institute, University of North Carolina at Chapel Hill, CB#7292, 9024 Burnett Womack, Chapel Hill, NC 27599. Phone: (919) 966-4026. Fax: (919) 843-6924. E-mail: cbrooke@med.unc.edu.

▽ Published ahead of print on 24 February 2010.

nisms involved in mediating recovery from VEEV-induced encephalomyelitis have been hampered by the lack of a relevant model system in which such a recovery could be reliably observed.

Using a fixed cDNA clone (pVR3000) of the Trinidad Donkey strain of VEEV as a starting point, our laboratory has generated a panel of genetically defined VEEV mutants that are attenuated *in vivo* compared to virus derived from the parental pVR3000 clone (1, 3, 12, 19, 60). The use of these mutants, which are attenuated at various definable stages of *in vivo* infection, has facilitated the dissection of the sequence of host-virus interactions that give rise to pathogenesis and/or immunity during VEEV infection (1, 3, 35). One of these laboratory-generated mutants, labeled V3533, differs from the parental V3000 virus at only two residues (E76K and K116E), both within the E2 glycoprotein, and yet these changes are sufficient to convert an invariably lethal virus into one that is nonlethal in immunocompetent C57BL/6 mice (1). Subcutaneous infection of C57BL/6 mice with V3533 resulted in neuroinvasion followed by rapid clearance. This reduction in pathogenicity did not result from an alteration of CNS cellular tropism, as both V3000 and V3533 exclusively infected neurons within the brain (data not shown). Thus, infection with V3533 provided a model system to study successful control of VEEV infection within the CNS.

In order to identify the components of a successful immune response to VEEV infection within the CNS, we infected a number of immunodeficient mouse strains with V3533 and assessed disease outcome. Infection of $Rag1^{-/-}$ mice with V3533 resulted in nearly total lethality, while infection of B cell-deficient μMT mice resulted in nearly total recovery, demonstrating that recovery from V3533 infection was dependent upon an adaptive immune response and that while antibody production contributed to recovery, it was not required. Further studies demonstrated that both $CD4^+$ and $CD8^+$ T cells had direct antiviral effects within the CNS and that both were required for maximal control of V3533 infection.

MATERIALS AND METHODS

Viruses. The isolation of wild-type V3000 and the V3533 mutant of VEEV, as well as the generation of the pVR3000 and pVR3533 molecular clones, has been described previously (1, 13). Virus stocks of V3533 were generated, using a T7-specific mMessage mMachine *in vitro* transcription kit (Ambion), by *in vitro* transcription from a linearized plasmid, pVR3533, which encodes the full-length V3533 cDNA. *In vitro*-generated transcripts were then electroporated into BHK-21 cells by the use of a Bio-Rad electroporator as described previously (1). Culture supernatants were harvested 18 h after electroporation, clarified by centrifugation at 3,000 rpm for 20 min, and stored as single-use aliquots at −80°C. Viral titers were determined by standard plaque assays on BHK-21 cells, as previously described (53).

Mouse studies. $Rag1^{-/-}$ and μMT mice (both on the C57BL/6 background) were obtained from the Jackson Laboratory (Bar Harbor, ME) and bred in-house under specific-pathogen-free conditions. C57BL/6 mice were purchased from the Jackson Laboratory as needed. All experimental manipulation of mice was performed in a biosafety level 3 animal facility following a 7-day acclimatization period. For infections, 6-to-10-week-old female mice were anesthetized via intraperitoneal (i.p.) injection with a mixture of ketamine (50 mg/kg of body weight) and xylazine (15 mg/kg of body weight) and then inoculated in the left rear footpad with 10^3 PFU of virus in diluent (phosphate-buffered saline [PBS], 1% donor calf serum, Ca^{2+}, Mg^{2+}). Mock-infected mice received diluent alone. Weight loss and disease score were assessed daily for infected animals. The scale used for disease scoring was as follows: 0, no signs of disease; 1, hunching; 2, ruffled fur; 3, ataxia, imbalance; 4, conjunctivitis; 5, paralysis of one or both hind limbs; and 6, moribund. This scale was based on the temporal order of ascending symptoms in μMT mice following V3533 infection. Mice that lost more than 20% (following V3000 infection) or 35% (following V3533 infection) of their starting weight or became moribund were euthanized according to University of North Carolina (UNC) Institutional Animal Care and Use Committee (IACUC) guidelines.

Virus titers. To assess VEEV titers *in vivo*, infected mice were sacrificed, bled, and then perfused through the heart with 10 ml of PBS. Spleen, draining popliteal lymph node, brain, and spinal cord tissues were then removed, weighed, and frozen in diluent at −80°C. Tissues were then thawed, homogenized, and used to infect BHK-21 cells in a standard plaque assay.

In vivo depletions. μMT mice received i.p. injections of 0.5 mg of depletion antibody in 0.1 ml of PBS 24 h prior to V3533 infection, 24 h following infection, and every 72 h subsequently until the termination of the experiment at day 25 postinfection. The depleting antibodies used were 17A2 (αCD3), GK1.5 (αCD4), 2.43 (αCD8), and LTF2 (isotype control) (all Bio X Cell). At day 25 postinfection, mice were bled and then sacrificed by exsanguination. Brains and spinal cords were collected for titering as described above, and spleens were collected to assess depletion efficacy by flow cytometry.

Quantification of CNS leukocytes and flow cytometry. Mock- and V3533-infected mice were sacrificed by exsanguination and perfused with PBS. Brains and spinal cords were harvested, minced, and then incubated for 1.5 h with vigorous shaking at 37°C in digestion medium (RPMI medium, 1% fetal calf serum, 25 mM HEPES, 1.25 mg/ml collagenase A [Roche]). Homogenates were then passed through a 40-μm-pore-size strainer and pelleted through 25% Percoll (GE Healthcare) in medium (RPMI medium, 1% fetal calf serum, 25 mM HEPES) for 20 min at 800 × *g*. The resulting pellets were then resuspended in 30% Percoll, overlaid above 70% Percoll, and centrifuged for 20 min at 800 × *g*. The interface was collected and washed with media, and the absolute number of live cells in each sample was then determined by trypan blue exclusion. Cells were washed in flow cytometry wash buffer (1× Hanks' balanced salt solution, 1% fetal calf serum, 0.1% sodium azide) and then stained with the following antibodies: anti-CD45-biotin coupled with streptavidin-conjugated PerCP, anti-anti-CD11b–phycoerithrin–Cy7 (anti-CD11b–PE–Cy7), anti-major histocompatibility complex class II–allophycocyanin (anti-MHC class II-APC), anti-Ly6G-fluorescein isothiocyanate (anti-Ly6G-FITC) (clone 1A8), and anti-CD3ε-PE (all eBioscience) and anti-CD4-Pacific Blue and anti-CD8-Pacific Orange (both Caltag). All staining was done in the presence of anti-mouse FcγRII/III (clone 2.4G2; BD Pharmingen) to prevent nonspecific antibody binding. Following staining, samples were fixed in 2% paraformaldehyde–PBS and analyzed using a CyAn flow cytometer and Summit 5.2 software (Dako). Absolute numbers of each specific cell type were calculated by determining the total number of live cells within a sample by trypan blue exclusion and then multiplying that number by the percentage of live cells within the sample bearing the appropriate surface staining profile.

***ex vivo* analysis of CNS leukocytes.** Leukocytes were isolated as described above. For samples receiving no *ex vivo* stimulus, cells were cultured in T cell culture media (RPMI medium, 10% fetal calf serum, 50 μM β-mercaptoethanol) with 3 μg/ml brefeldin A (eBioscience) for 4 h at 37°C. For samples receiving stimulus, cells were cultured in T cell culture media with 50 ng/ml phorbol myristate acetate (PMA) and 500 ng/ml ionomycin for 6 h at 37°C, with brefeldin A added for the last 4 h. CD107a staining was performed during brefeldin A treatment, in the presence of 2 μM monensin and 1:100 anti-CD107a-AF488 or an isotype control (eBioscience). Cells were then washed in flow cytometry wash buffer and stained with the following antibodies: anti-CD69-PE-Cy5 and anti-CD3ε-PE (both eBioscience) and anti-CD4-Pacific Blue and anti-CD8-Pacific Orange (both Caltag). Following surface staining, cells were washed twice and then simultaneously fixed and permeabilized in Cytofix/Cytoperm (BD Biosciences) for 30 min. Permeabilized samples were stained for intracellular expression using the following antibodies: anti-Ki-67–FITC, anti-IFN-γ–PE–Cy7, anti-TNF-α–FITC, anti-IL-2–APC, anti-IL-10–APC, anti-IL-17–APC, or the appropriate isotype controls (all eBioscience). All staining was done in the presence of anti-mouse FcγRII/III (2.4G2; BD Pharmingen) to prevent nonspecific antibody binding. Samples were then washed twice in Cytoperm/Cytowash (BD Biosciences) and then analyzed on a CyAn flow cytometer.

RESULTS

V3533 provides a relevant model of viral clearance and recovery. Following subcutaneous, footpad injection of C57BL/6 mice with 10^6 PFU of V3533, the early stages of viral replication and spread were similar to those observed previ-

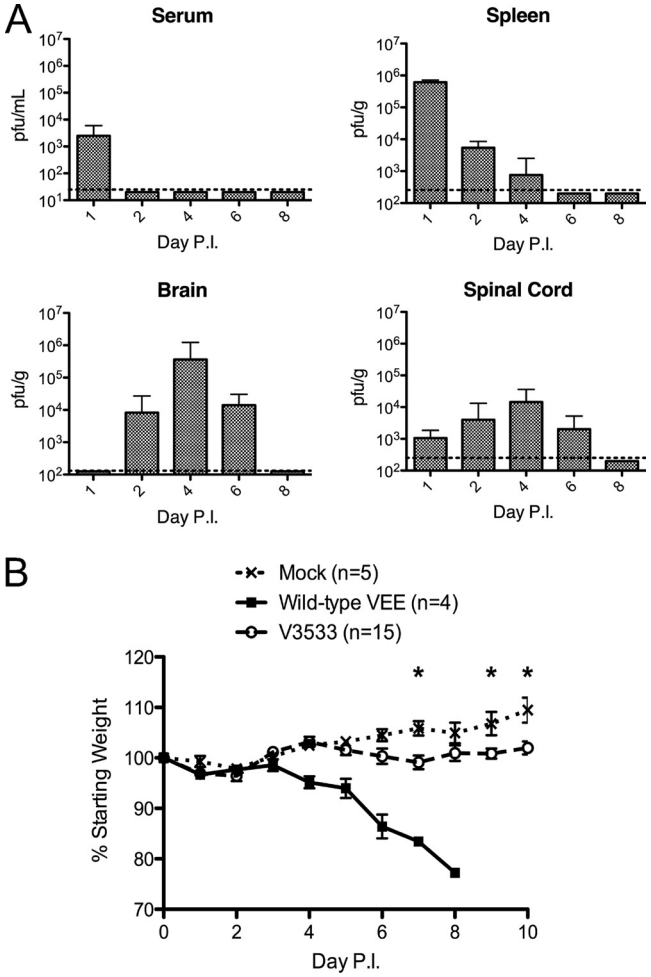

FIG. 1. V3533 induces mild, transient disease followed by clearance in C57BL/6 mice. (A) Female C57BL/6 mice (7 to 10 weeks old) were inoculated with 10^6 PFU of V3533 by injection in the left rear footpad. At the indicated days postinfection (Day P.I.), serum, spleen, brain, and spinal cord samples were collected from V3533-infected mice and homogenized. The amount of infectious virus present in serum, spleen, brain, and spinal cord samples was then quantified by plaque assays of BHK-21 cells. Data are presented as the means ± standard deviations of results pooled from two independent experiments with 3 to 10 animals per time point. Dotted lines represent the limit of detection. (B) Female C57BL/6 mice (7 to 10 weeks old) were inoculated with 10^3 PFU of wild-type VEEV (V3000) or 10^6 PFU of V3533 by injection in the left rear footpad. Mock-infected mice were infected with diluent alone. Mice were weighed daily, with those losing more than 20% of their starting weight being euthanized as required by UNC IACUC regulations. *, $P < 0.05$ by Mann-Whitney testing.

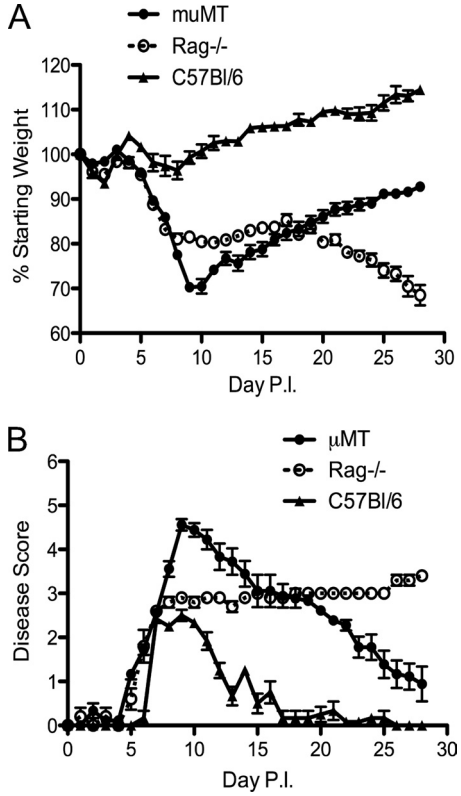

FIG. 2. Rag1$^{-/-}$ mice succumb to V3533 infection, whereas μMT mice recover. Female μMT or Rag1$^{-/-}$ mice (7 to 10 weeks old) were inoculated with 10^3 PFU of V3533 by injection in the left rear footpad. C57BL/6 mice received 10^6 PFU of V3533. (A) Mice were weighed daily, with those losing more than 35% of their starting weight being euthanized as required by UNC IACUC regulations. (B) Mice were scored for the development of encephalomyelitis based on the following scale: 1, hunched posture; 2, ruffled fur; 3, ataxia, imbalance; 4, conjunctivitis; 5, hind limb paresis, paralysis; 6, moribundity. Each data point represents the mean ± standard error of the mean (SEM) of the results obtained with 6 animals per group from a single representative experiment.

ously with the more virulent parental virus, V3000 (Fig. 1A and data not shown) (19). Virus in the draining popliteal lymph node, spleen, and serum was first observed by 24 h postinfection. The virus first became detectable in the brain by a plaque assay at day 2 postinfection, while titers in secondary lymphoid organs and serum were reduced considerably by this time point. Viral titers peaked within the CNS around day 4, but unlike wild-type virus that maintained high titers within the CNS until the inevitable death of the host (data not shown), titers of V3533 began to decline by day 6, and by day 8, infectious virus was no longer detectable by plaque assay. Replication of V3533 within the CNS was associated with a small but significant loss of weight relative to the results seen with mock-infected mice in multiple independent experiments (Fig. 1B and 2). Upon clearance, infected mice began regaining weight and eventually stopped exhibiting outward signs of disease. Thus, V3533 provides a model of VEEV infection in which the host is able to successfully clear the virus from the CNS and recover from clinical illness.

Antibody production is not required for recovery from V3533-induced encephalomyelitis. The role of the adaptive component of the immune system in mediating protection or recovery during VEEV infection has been tested primarily in the context of vaccinated animals or animals receiving passive transfer of immune sera. While these studies have been instructive, we were interested in what role the adaptive response could play during the infection of a naïve animal. To answer this question, we determined whether the observed control of V3533 by C57BL/6 mice was dependent on the adaptive arm of the immune system.

Rag1$^{-/-}$ mice, which lack functional B and T cells, as well as

μMT mice, which lack functional B cells, were infected with 10^3 PFU of V3533 subcutaneously in the footpad. Rag1$^{-/-}$ mice initially behaved similarly to wild-type mice, losing little or no weight and showing no outward signs of disease for the first 4 days postinfection (Fig. 2). At day 4, infected Rag1$^{-/-}$ mice began losing weight and by day 8 postinfection had lost roughly 20% of their starting weight. They also developed clinical signs of disease, including hunched posture, ruffled fur, ataxia, and a marked reduction in cage exploration. Weight loss and clinical signs of disease in infected Rag1$^{-/-}$ mice progressed rapidly between days 4 and 8 postinfection, but the clinical condition of the animals then stabilized, and over the next 10 days both weight and clinical score remained virtually unchanged. Starting around day 18 postinfection, however, infected Rag1$^{-/-}$ mice suffered further weight loss, culminating in death. V3533 infection of Rag1$^{-/-}$ mice resulted in 93% lethality ($n = 15$) over 40 days of observation, with an average survival time (AST) of 30 ± 5 days. The differences in disease outcome observed between C57BL/6 and Rag1$^{-/-}$ mice clearly demonstrated that successful control of V3533 infection is dependent upon an intact adaptive immune response.

The importance of an intact antibody response was demonstrated by following V3533 infection of μMT mice. Between days 4 and 9 postinfection, μMT mice lost about 30% of their starting weight and developed the outward signs of severe encephalomyelitis, including convulsions, conjunctivitis, and hind-limb paresis or paralysis. This dramatically enhanced pathology, compared with the much milder disease observed in wild-type mice, illustrated the critical role that antibody production played in mounting a successful response to VEEV infection. Surprisingly, despite the extremely severe morbidity observed, the vast majority (92.7% [64/69]) of these animals went on to recover. Recovery of μMT mice was somewhat protracted, with mice not regaining their full starting weights until weeks later. Most outward signs of encephalomyelitis or febrile illness disappeared in recovered μMT mice, though these animals retained a slight tentativeness in their movements that was still observable 15 weeks after infection. The stark contrast in disease outcome following V3533 infection in μMT mice versus Rag1$^{-/-}$ mice clearly demonstrated that other adaptive mechanisms in addition to antibody production could play a major protective role during VEEV infection.

Recovery in μMT mice is associated with dramatic reduction of viral titers in the brain and clearance of infectious virus in the spinal cord. Persistent CNS infection by wild-type VEEV in mice has not been previously reported. The unexpected recovery observed in V3533-infected μMT mice led us to ask whether the observed recovery was associated with clearance of virus from the CNS or the establishment of viral persistence. To answer this question, we infected μMT mice subcutaneously in the footpad with 10^3 PFU of V3533 and then sacrificed animals at various times postinfection and assessed viral burden in relevant tissues by plaque assay.

The pattern of early V3533 replication and dissemination observed in μMT mice differed somewhat from the classic biphasic course of infection that has previously been seen in VEEV-infected immunocompetent mice (1). Virus was first seen in the draining popliteal lymph node within 12 h of inoculation and in the spleen and serum by 24 h. Rather than being rapidly cleared from these compartments, as is the case with C57BL/6 mice, infectious V3533 remained detectable in both serum and spleen for weeks following inoculation (Fig. 3A). Of 6 mice examined at 15 weeks postinfection, virus was still detectable in serum (4/6) and spleen (2/6) by plaque assay (Fig. 3B).

V3533 first appeared in the brains of μMT mice around 24 h postinfection and rapidly reached peak titers of around 10^6 PFU/g by day 4. The appearance of virus in the spinal cord was slightly delayed, with infectious virus first detectable at 48 h postinfection and peak titers being reached at day 6 (Fig. 3A). Thus, the kinetics of neuroinvasion and initial replication of the virus within the CNS were similar to those observed in C57BL/6 mice. Between days 6 and 8, however, titers in both brain and spinal cord began to fall and by day 15 postinfection had been reduced to within 1 log of the limit of detection. Following this initial reduction of viral titers within the CNS, infectious virus was cleared from the spinal cord between days 15 and 30 postinfection but continued to persist in the brains of the majority of animals tested through week 15 (day 105), indicating the development of a chronic infection (Fig. 3B). This divergence in the abilities of the brain and spinal cord to clear virus in the absence of antibody mirrors what has been reported previously in a study of Sindbis virus infection in these mice (5).

Given that μMT mice were able to control V3533 infection within the CNS and recover from infection, we next asked whether the mortality observed in V3533-infected Rag1$^{-/-}$ mice was due to an inability to control viral replication. To answer this question, we directly compared both systemic and CNS titers between μMT and Rag1$^{-/-}$ mice at days 6 and 25 following subcutaneous infection with 10^3 PFU of V3533. While viral titers were high at day 6 postinfection in both μMT and Rag1$^{-/-}$ mice, by day 25 μMT mice were able to reduce titers in both serum and the brain substantially, while Rag1$^{-/-}$ mice continued to maintain extremely high titers in both tissues, potentially explaining the enhanced mortality rate in these mice (Fig. 3C).

Reduction in viral CNS titers occurs concurrently with an influx of inflammatory monocytes and T cells. The dramatic reductions in CNS titers in the absence of antivirus antibody led us to ask which immune cell populations were responsible. We first identified leukocyte populations present in the brains and spinal cords of V3533-infected mice over the course of infection. μMT mice were infected subcutaneously in the footpad with 10^3 PFU of V3533. At different times postinfection, infected animals were sacrificed and CNS-infiltrating leukocytes were isolated. Different leukocyte populations were then identified by surface phenotype and quantified by flow cytometry (Fig. 4A).

The vast majority of leukocytes in the uninfected CNS were identified as resting microglia, defined as CD11b$^+$ CD45^{lo} MHC class II^{lo}, with minimal numbers of other populations being detectable (17, 49). Following invasion of the CNS by V3533, however, this picture changed dramatically. Between days 4 and 10 postinfection, a massive expansion in a CD11b$^+$ CD45^{hi} Ly-6G$^-$ MHC class II^{hi} population, defined as inflammatory monocytes, was observed (16, 29, 49). This population increased in both number and activation state, as assessed by MHC class II expression, over this time period (Fig. 4B and data not shown) (55). Between days 6 and 10 postinfection, the

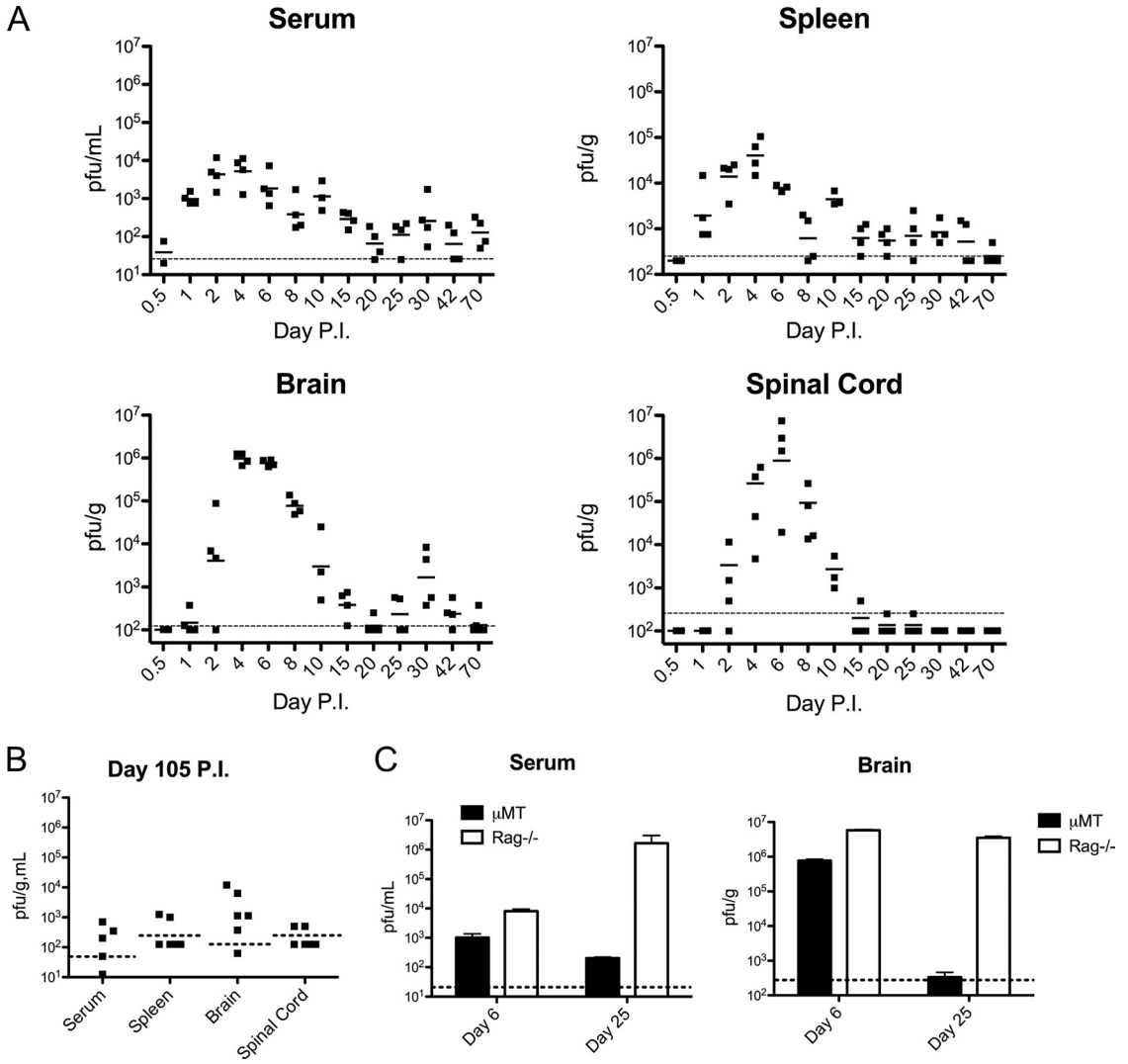

FIG. 3. Recovery in μMT mice is associated with control of viral replication in the brain and clearance in the spinal cord. Female μMT or Rag1$^{-/-}$ mice (7 to 10 weeks old) were inoculated with 10^3 PFU of V3533 by injection in the left rear footpad. (A) At the time points indicated, serum, spleen, brain, and spinal cord samples were collected from infected μMT mice and homogenized. The amount of infectious virus present in the serum, spleen, brain, and spinal cord samples was then quantified by plaque assays of BHK-21 cells. Data points represent individual tissue titers pooled from two independent experiments. (B) Tissue titers from infected μMT mice at day 105 postinfection. (C) Comparison of tissue titers between μMT and Rag1$^{-/-}$ mice. Data are presented as the means ± SEM of titer values from 3 to 4 animals per group. In all cases, dotted lines represent the limit of detection.

numbers of CD4$^+$ and CD8$^+$ T cells within the CNS increased from barely detectable to 10^6 cells/brain and 10^5 cells/spinal cord. After peaking at day 10, these inflammatory cell populations began rapidly contracting, with inflammatory monocytes and T cell populations exhibiting a 5-to-10-fold decrease in numbers by day 15 postinfection (Fig. 4B). Interestingly, the period during which infected μMT mice exhibited increasingly severe disease signs and weight loss corresponded in time precisely to the period during which inflammatory monocytes and T cell numbers within the CNS expanded, while the onset of recovery in those animals corresponded to the contraction of those cell populations (Fig. 2).

Due to the persistence of low levels of infectious virus in the brains of recovered μMT mice, we asked whether different inflammatory cell populations were retained in the CNS during the chronic phase of the infection. Comparing total cell numbers in the brains of μMT mice 70 days after infection with V3533 with those from mock-infected μMT mice, we found significantly elevated numbers of inflammatory monocytes and CD4$^+$ and CD8$^+$ T cells, but not microglia, in the infected group. In the spinal cord samples, all cell populations tested were significantly elevated above mock-infection levels (Fig. 4C; $P < 0.05$ [Mann-]Whitney). Additionally, microglia and inflammatory monocytes from the persistently infected mice showed significantly higher levels of MHC class II staining relative to mock-infection levels, indicating that they retained an activated phenotype ($P = 0.0286$ [Mann Whitney]; data not shown).

T cells are required for control of V3533 infection and recovery in μMT mice. Numerous findings from studies demon-

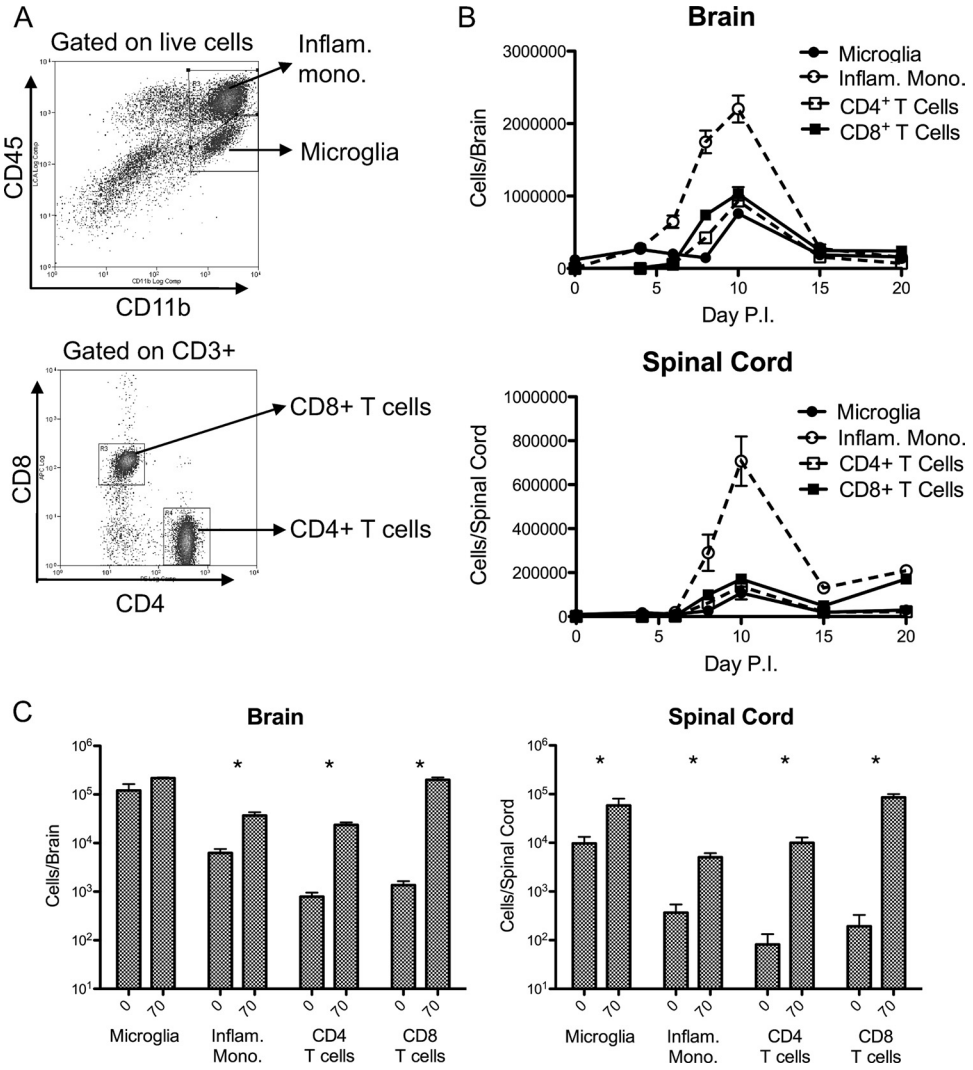

FIG. 4. Reduction of viral titers in the CNS coincides with an influx of T cells and inflammatory monocytes. Female μMT mice (7 to 10 weeks old) were inoculated with 10^3 PFU of V3533 or diluent alone by injection in the left rear footpad. At various time points postinfection, mice were perfused with PBS and CNS-infiltrating leukocytes were isolated. Infiltrating cells were stained for various surface markers and analyzed by flow cytometry. (A) Representative dot plots illustrating the gating scheme used to define cell populations. (B) Total numbers of microglia ($CD11b^+/CD45^{lo}$), inflammatory monocytes ($CD11b^+/CD45^{hi}$), $CD4^+$ T cells ($CD3^+/CD4^+$), and $CD8^+$ T cells ($CD3^+/CD8^+$) isolated from brain and spinal cord samples. For each time point, data are presented as the means ± the standard errors of the results obtained with 3 to 4 mice and are representative of 2 independent experiments. (C) Comparison of total cell numbers of indicated infiltrating leukocyte populations between mock-infected mice (left bar) and V3533-infected mice (right bar) 70 days postinfection. Data are presented as means ± standard errors of the results obtained with four animals per group. *, $P < 0.05$ by Mann-Whitney testing.

strating the importance of T cells in mediating antiviral immunity in other viral systems, as well as the dramatic difference in survival rates between μMT and $Rag1^{-/-}$ mice that we observed, suggested that T cells are required for the recovery observed in V3533-infected μMT mice. It was also possible that the relative contributions of $CD4^+$ and $CD8^+$ populations to control of the infection and recovery differed. To address these questions, we treated μMT mice with depleting antibodies against CD3, CD4, or CD8 or with an isotype control antibody. Weight loss and disease score were observed for 25 days following infection, at which point surviving mice were sacrificed and assayed for viral burden in the CNS as well as in serum. The efficacy of the depletion treatments was also assessed at the termination of the experiment by flow cytometric analysis of splenocytes (Fig. 5A).

In terms of disease outcome, the antibody isotype control group was indistinguishable from the untreated μMT mouse group following V3533 infection, with animals developing the same overt signs of severe encephalomyelitis and then recovering (Fig. 2 and 5B). The CD3-depleted group immediately began exhibiting signs of illness upon infection, including weight loss, hunching, ruffling, and ataxia. These disease signs closely mirrored what was observed in V3533-infected $Rag1^{-/-}$ mice, without the convulsions, conjunctivitis, and hind limb paresis observed in infected μMT mice. Also, in similarity to the disease observed in $Rag1^{-/-}$ animals, illness in

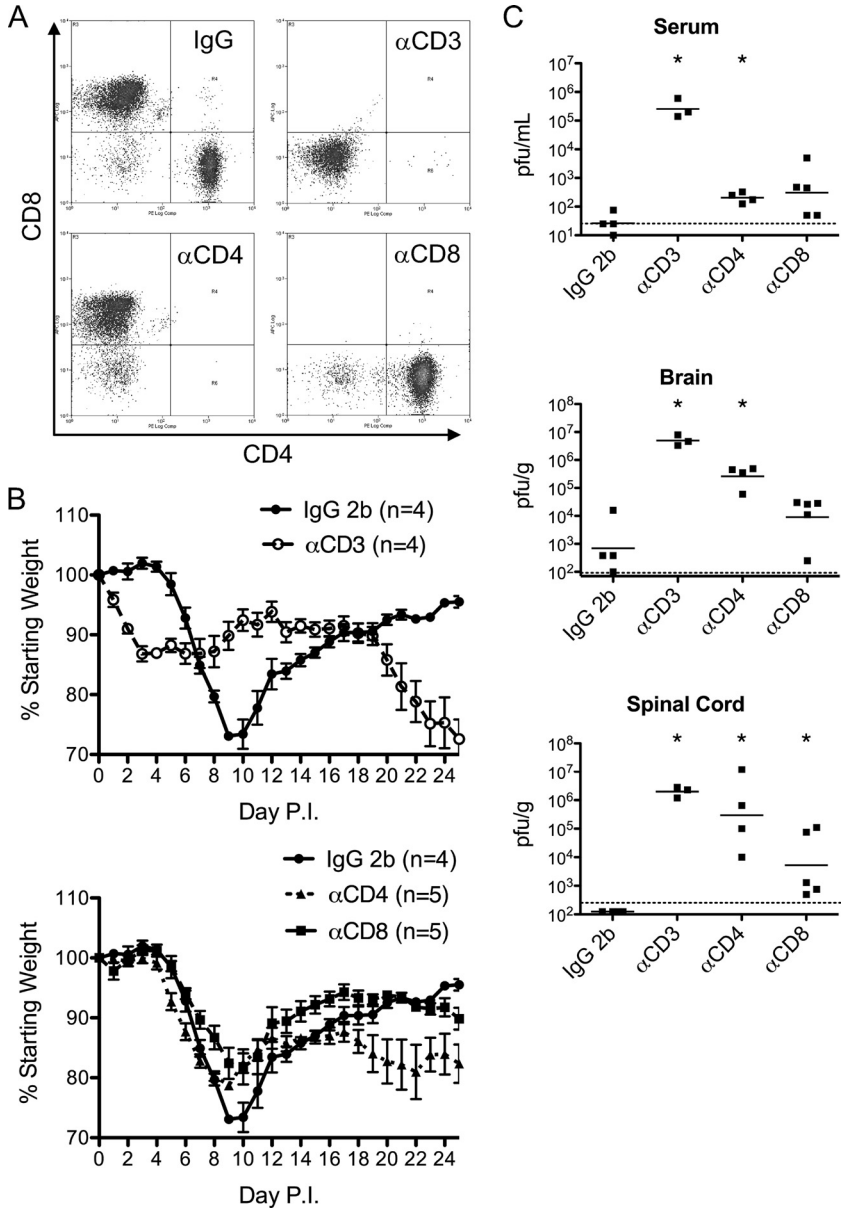

FIG. 5. T cells are required for control of infection and recovery in μMT mice. Female μMT mice (7 to 10 weeks old) were treated with depleting antibodies against CD3, CD4, or CD8 or with an isotype control antibody and then inoculated with 10^3 PFU of V3533 by injection in the left rear footpad. Depletion treatments were continued for 25 days postinfection, at which point the experiment was terminated. (A) Representative dot plots of $CD3^+$ splenocytes from each group, taken at day 25 postinfection. (B) Effect of T cell depletions on weight loss following V3533 infection. Data represent means ± standard errors of the results obtained with 4 to 5 animals per group. (C) Infectious virus from tissues harvested 25 days postinfection, assessed by plaque assays on BHK-21 cells. Each data point represents a single animal, with bars indicating the geometric means. *, $P < 0.05$ compared to control by Mann Whitney testing.

the CD3-depleted group was prolonged but generally sublethal, with 3 of 4 animals still alive at the termination of the experiment at day 25 postinfection. Those surviving animals appeared to be nearing death, however, suggesting that lethality would have been 100% had the experiment been allowed to continue. The one significant difference observed between the CD3-depleted group and $Rag1^{-/-}$ mice was that the onset of disease was much more rapid in the CD3-depleted group, with signs of fever and weight loss easily observable by 24 h postinfection (Fig. 2 and 5B and data not shown). This was most likely not an artifact of the depletion, as both the CD4- and CD8-depleted groups exhibited the same delay between infection and disease onset as untreated μMT mice.

In order to more directly examine the role of T cells in controlling V3533 infection in μMT mice, we compared viral burdens at 25 days postinfection both within the CNS and systemically between the different depleted groups with those in the control group (Fig. 5C). As expected, based on infection of untreated μMT mice, the antibody isotype control-treated group showed low to undetectable viral burdens in the brain

and serum and no detectable infectious virus in the spinal cord. The CD3-depleted mice, however, demonstrated a complete inability to control the infection, with titers in all three compartments tested ranging from 10^5 PFU/ml in the serum to 10^7 PFU/g in the brain. These results clearly demonstrated a requirement for the T cell compartment in controlling V3533 infection in the absence of antibody.

Both $CD4^+$ and $CD8^+$ T cells are required for effective control of V3533 infection in μMT mice. Initial disease severity in both CD4- and CD8-depleted groups appeared to be somewhat intermediate between the levels of severity seen with the control and CD3-depleted groups. During the time of peak disease severity (days 9 to 10), both the CD4- and CD8-depleted groups lost significantly less weight than the antibody isotype control-treated group ($P < 0.05$ [Mann-Whitney]), and neither group developed the conjunctivitis and/or hind limb paresis that were characteristic of V3533 infection in untreated μMT mice (Fig. 5B and data not shown). This indicated that both $CD4^+$ and $CD8^+$ T cells together were required for the most extreme pathology observed in μMT mice following V3533 infection.

While the CD4 and CD8 depletion treatments reduced the severity of V3533-induced disease during the early stages of infection, they also appeared to reduce the ability of those animals to recover compared with the control group (Fig. 5B). At the termination of the experiment, 25 days postinfection, one of five CD4-depleted mice had already succumbed to infection, and the survivors were steadily losing weight, indicating that they were not successfully controlling the infection. The CD8-depleted group, while appearing to have recovered more fully than the CD4-depleted group at first, also had begun to deteriorate again by the end of the experiment, resulting in significantly lower weights and significantly higher disease scores compared with the antibody isotype control group at day 25 (both $P < 0.05$ [Mann-Whitney]). Although the experiment was not extended long enough to determine final survival rates for the different groups, the status of the CD4- and CD8-depleted groups at the termination of the experiment strongly suggested that both $CD4^+$ and $CD8^+$ T cell populations were required for complete recovery from V3533 infection.

Having established the necessity of T cells for effective control of V3533 and recovery, the relative contributions of the $CD4^+$ and $CD8^+$ compartments to the control of the virus both systemically and within the CNS were determined (Fig. 5C). In the serum at day 25 postinfection, mean virus titers in both the CD4- and CD8-depleted groups were roughly 3 logs lower than in the CD3-depleted group, though still elevated above those in the antibody isotype control group, indicating that each population was able to exert substantial control over systemic replication of V3533 and that both populations were required for maximal control. In brain tissue, mean virus titers in mice depleted of $CD8^+$ cells were statistically indistinguishable from those of the antibody isotype control group ($P = 0.1761$ [Mann-Whitney]). Brain titers in the CD8-depleted group were significantly lower than in the CD3-depleted group, however ($P = 0.0357$ [Mann-Whitney]). In the CD4-depleted group, titers were significantly elevated above those seen with both the control and the CD8-depleted groups ($P = 0.0294$ and 0.0159, respectively [Mann-Whitney]) but were indistinguishable from those seen with the CD3-depleted group ($P = 0.0571$ [Mann-Whitney]). In spinal cord tissue, we observed a similar trend in which titers in CD8-depleted mice were significantly lower than those of the CD3-depleted group but titers in CD4-depleted mice were not statistically distinguishable from those in the CD3-depleted group ($P = 0.4$ and $P = 0.0357$, respectively [Mann-Whitney]) (Fig. 5C). Together, these results suggest that within the CNS, the $CD4^+$ compartment contributes the majority of the T cell-associated antiviral activity and that both $CD4^+$ and $CD8^+$ cells are required for maximal control.

$CD4^+$ T cells are the primary source of T cell-associated IFN-γ within the brain. The apparent differences in antiviral activity observed between $CD4^+$ and $CD8^+$ cells within the CNS might be explained by differences in expression of cytokines or other indicators of effector function. To address this possibility, we isolated T cells from the brains of V3533-infected μMT mice at days 8, 15, and 70 postinfection and assessed expression of IFN-γ, TNF-α, IL-2, IL-10, and IL-17 by intracellular cytokine staining. We also looked at surface expression of CD69 and CD107a as markers of recent activation and degranulation, respectively. Day 8 was chosen to provide a snapshot of T cell behavior during the peak of antiviral activity, as T cell numbers in the CNS were increasing and viral titers were decreasing at this time. Day 15 represented a point after which both viral titers and T cell numbers within the CNS had decreased substantially and recovery had begun. Day 70 was chosen to represent a point well into the chronic phase of infection.

T cell behavior within the brains of V3533-infected mice was determined using two complementary approaches. The first was to nonspecifically stimulate brain-infiltrating T cells with PMA and ionomycin for 6 h *ex vivo* prior to flow cytometric analysis to determine how these cells were capable of responding (Fig. 6A). Using this approach, it appeared that $CD4^+$ and $CD8^+$ cells were programmed to respond similarly to V3533 infection within the brain. Large numbers of IFN-γ- and TNF-α-producing $CD4^+$ and $CD8^+$ cells were detected whereas IL-17- and IL-10-producing cells were much less prevalent, indicating that both the $CD4^+$ and $CD8^+$ cell populations appeared to be participating in a predominantly Th1-skewed response. IL-2 production was minimal, in accordance with previous findings for Sindbis infection (26). The numbers of IFN-γ- and TNF-α-producing $CD4^+$ and $CD8^+$ cells were roughly equivalent at day 8, but by day 15 the number of $CD8^+$ cells producing both cytokines was approximately 2-fold higher than the number of $CD4^+$ cells producing both cytokines, reflecting an overall increase in the ratio of total $CD8^+$ cells to $CD4^+$ cells at this time point. At all time points, a higher percentage of $CD8^+$ cells than $CD4^+$ cells stained positive for surface expression of the recent degranulation marker CD107a. These results suggest that brain-infiltrating $CD4^+$ and $CD8^+$ T cells were similar in their abilities to produce IFN-γ and TNF-α *ex vivo* during the acute phase response to V3533 and that the degranulation activity of $CD8^+$ T cells was superior to that of $CD4^+$ cells. Both $CD4^+$ and $CD8^+$ T cells retained multiple effector capabilities well into the chronic phase of VEEV infection, indicating that the phenomenon of T cell exhaustion was not occurring in this system (Table 1). The caveat with results obtained by PMA-ionomycin treatment, however, is that they represent only how T cells are

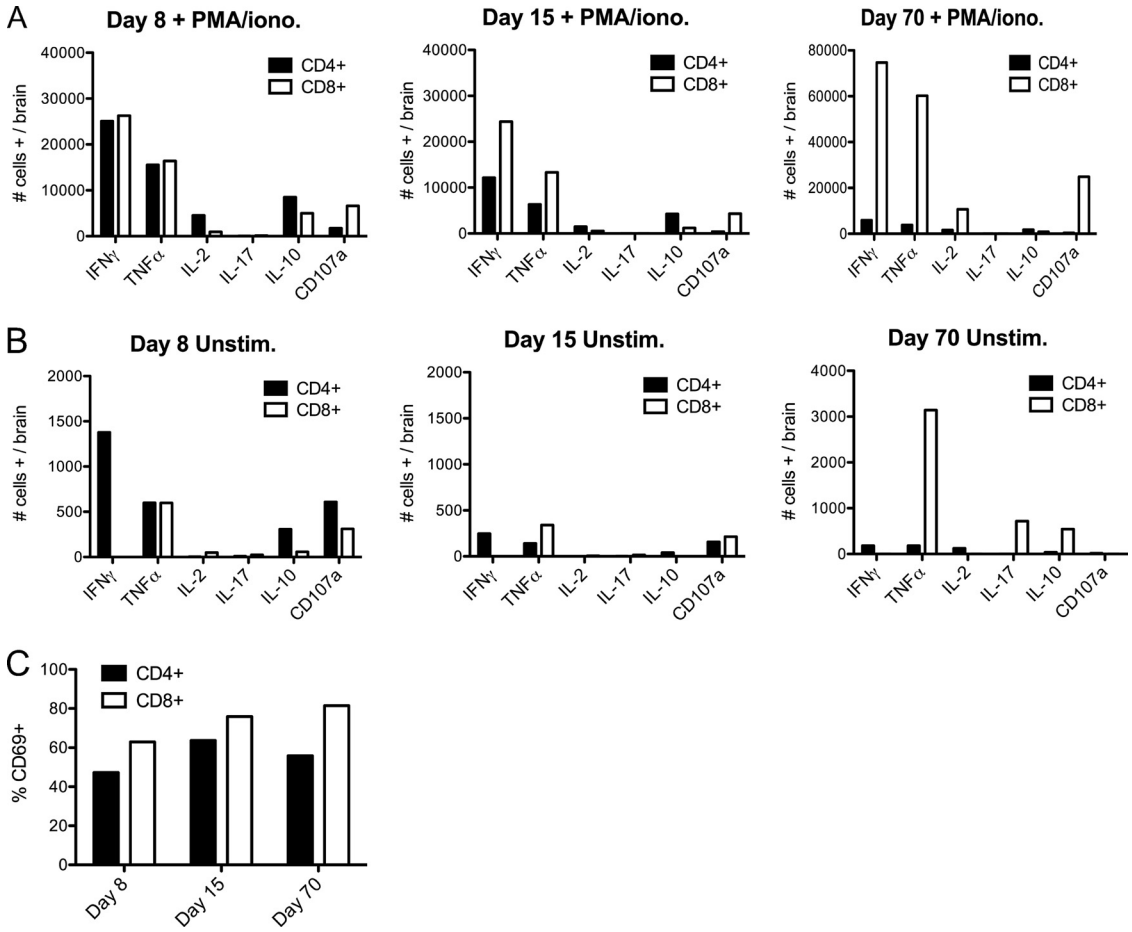

FIG. 6. $CD4^+$ T cells are the main producers of T-cell-associated IFN-γ within the brains of V3533-infected μMT mice. Female μMT mice (7 to 10 weeks old) were inoculated with 10^3 PFU of V3533 by injection in the left rear footpad. At the times indicated, mice were perfused with PBS and brain-infiltrating leukocytes were isolated. (A and B) Harvested cells were then pooled and either cultured in the presence of PMA-ionomycin for 6 h with brefeldin A with or without monensin added for the final 4 h (A) or cultured in the presence of brefeldin A with or without monensin with no additional stimulus for 4 h (B). Following treatment, cells were surface stained for CD3α, CD4, and CD8 and then stained for the intracellular presence of multiple cytokines. Each bar represents the number of cells of a given cell type that stained as positive for the indicated cytokine-surface marker per brain (days 8 and 15) or the percentage of pooled cells that stained as positive (day 70). (C) Percentages of T cells positive for CD69 surface expression in the absence of *ex vivo* stimulation. Data shown were generated in a single experiment but are representative of 2 to 3 independent experiments.

programmed to respond but not how they actually behave *in vivo*.

A second approach gave a more direct measurement of how T cells were actually behaving *in vivo*. Rather than being treated with PMA and ionomycin following isolation, brain-infiltrating T cells were treated only with brefeldin A, with or without monensin, prior to flow cytometric analysis (Fig. 6B). No external stimulus was provided. While this treatment probably resulted in artificially low levels of detectable expression due to the time lag between sacrifice of the animal and cell fixation, we feel that any results observed using this method were the direct result of the stimuli and regulatory signals present within the brains of V3533-infected mice. Brain-infiltrating T cells analyzed in the absence of *ex vivo* stimulus exhibited a dramatically different pattern of IFN-γ and CD107a expression compared to that observed following PMA-ionomycin treatment. At days 8, 15, and 70 postinfection, significant IFN-γ expression was detectable only within the $CD4^+$ population. IFN-γ-positive $CD8^+$ T cells were undetectable at all time points. In addition, a larger percentage of $CD4^+$ cells expressing surface CD107a than of $CD8^+$ cells was detected during the acute phase. Finally, IL-2-, IL-17-, and IL-10-expressing cells were sparse in both

TABLE 1. Percentages of brain-infiltrating T cells expressing the indicated cytokines at day 70 postinfection

Cytokine	% $CD4^+$ cells		% $CD8^+$ cells	
	PMA-ionomycin stimulation	No stimulation	PMA-ionomycin stimulation	No stimulation
IFN-γ	62.03	1.92	77.96	0.0
TNF-α	40.51	1.92	62.84	3.28
IL-2	16.91	1.32	11.19	0.0
IL-17	0.0	0.0	0.0	0.75
IL-10	18.75	0.4	0.93	0.57
CD107a	4.81	0.2	26.01	0.0

$CD4^+$ and $CD8^+$ T cells. Together, these results indicate that during the acute phase of the response to V3533 infection within the brain, $CD4^+$ T cells produced more IFN-γ and had higher levels of degranulation activity than $CD8^+$ T cells, potentially explaining why these cells exhibited anti-VEEV activity of greater potency.

While the lack of known T cell epitopes prevented us from directly examining VEEV-specific T cells, we felt that the use of CD69 staining provided a reasonable alternative. CD69 expression on T cells serves as a marker of recent encounter with cognate antigen and should not be expressed on bystander T cells (47). At each time point examined, $CD69^+$ cells constituted roughly 50 to 80% of all $CD4^+$ and $CD8^+$ T cells within the brain (Fig. 6C). This is consistent with the majority of brain-infiltrating T cells being VEEV-specific during both the acute and chronic phases of infection.

DISCUSSION

While the important protective role of B cells and virus-specific antibodies during neuronotropic alphavirus infection has been well established, the role of T cells remains relatively ill defined. Work with avirulent Sindbis virus has suggested that T cells might directly act to limit viral infection within the CNS by noncytolytic mechanisms; however, the results of studies using virulent strains of Sindbis or VEEV were contradictory, suggesting instead that T cells might either act to enhance pathology or play no significant role whatsoever (5, 28, 44). Previous studies evaluating the immune response to VEEV infection have been hampered by the lack of a model system in which successful control of infection could be reliably observed. To better understand the role of T cells during a successful immune response to acute VEEV infection, we utilized V3533, a mutant of VEEV that is capable of invading the CNS from the periphery and yet only induces mild, transient disease in immunocompetent mice. We feel that this provides a more relevant model of the results of VEEV-induced disease in humans than the universal lethality observed in mice infected with wild-type VEEV strains, as natural infections of humans very rarely progress to overt encephalomyelitis and death (58). Using V3533 infection of mice as a model of successful recovery from VEEV-induced encephalomyelitis, we asked whether T cells played a significant role during recovery from VEEV infection, independent from any effect on antibody production. We observed that B cell-deficient μMT mice were able to recover from V3533 infection while T cell-depleted μMT mice were not, clearly demonstrating that T cells could facilitate clinical recovery from VEEV-induced encephalomyelitis in the absence of antibody.

We chose to carry out these studies using μMT mice, rather than B cell-depleted immunocompetent mice, in order to ensure that antibody production was completely absent. Given the highly protective effects that antibodies demonstrated in other alphavirus infection models, we were concerned that even a small percentage of endogenous B cells that survived a depletion treatment might exert enough of an effect to confound the potentially subtle T cell-associated effects in which we were interested (32). The use of μMT mice as "B cell-deficient" mice is complicated by the observation that these mice exhibit various T cell deficiencies relative to wild-type mice (2). We cannot rule out the possibility that these defects, which affect both expansion and function in $CD4^+$ and $CD8^+$ T cells, might contribute to the viral persistence that we observed. However, the fact that T cells are able to control V3533 infection and facilitate recovery in μMT mice despite these strain-specific deficiencies strengthens our conclusion that T cells contribute a significant antiviral effect during V3533 infection.

Viral infection of CNS neurons presents a unique problem for the immune system in that they are absolutely essential for host function and yet are not easily replaced (34). As a result, widespread immune-mediated cytolysis of infected cells can present a greater threat to host viability than the virus itself (10). In the case of infection with a highly virulent virus, the benefits of cytolytic clearance mechanisms might be worth the cost in enhanced pathology; however, it appears that the mammalian immune system has also evolved noncytolytic mechanisms of T cell-mediated clearance. In particular, studies with Sindbis virus, Theiler's murine encephalomyelitis virus (TMEV), and measles virus have all implicated T cell-associated IFN-γ production in mediating noncytolytic clearance of virus from infected neurons (7, 38, 42). The studies described here clearly demonstrated that, during V3533 infection, T cells were able to significantly restrict viral replication within the brain and clear infectious virus from the spinal cord, thus facilitating recovery from a severe viral encephalomyelitis. While this reduction in CNS titers was clearly associated with disease signs of greater severity than were observed in $Rag1^{-/-}$ mice, the rapid onset of recovery and the absence of long-lived sequelae within the brain suggest that control of the infection was not achieved simply by destruction of infected neurons.

The failure of μMT mice to fully clear infectious virus from the CNS mirrors what has been previously observed in μMT mice infected with Sindbis virus (5). The ability of these mice to recover from V3533-induced encephalomyelitis despite the continuing presence of infectious virus within the CNS as well as in the rest of the system raises a number of questions. The most obvious is this: what are the cellular reservoirs of virus that prevent total clearance? Studies with Sindbis virus have indicated that neuronal subpopulations within the CNS are differentially susceptible to IFN-γ-mediated clearance (8). Whether these differences are due to intrinsic differences in the IFN-γ-signaling network within these cells or to some other mechanism remains to be determined. If there is a stable reservoir of clearance-refractory neurons that are responsible for the observed persistence, how are those cells able to survive prolonged infection with a cytolytic virus? Despite the presence of robust antiapoptotic programming within mature neurons, virulent strains of VEEV are able to induce widespread neuronal death (10, 22, 27). It may be that V3533 is less efficient at overcoming these mechanisms, thus allowing long-term survival of infected neurons. If this is the case, understanding the molecular basis of this difference will be of great interest. Another issue that remains unresolved is the extent to which host neurological function is compromised by the ongoing persistent infection and accompanying low-level inflammatory response (40). While μMT mice appear to recover fully from V3533-induced clinical disease, it is possible that a more in-depth evaluation of cognitive function in the animals that recover might reveal subtle defects.

Given the continuing presence of infectious virus within the CNS of recovered μMT mice, it is not surprising that activated T cells were retained within the brain and spinal cord. What was somewhat surprising was that both $CD4^+$ and $CD8^+$ T cells retained functionality, as determined by IFN-γ expression, as long as 70 days following infection. The loss of T cell function, specifically IFN-γ expression, has been well documented in other models of persistent viral infection and is thought to result from prolonged antigen exposure (6, 36, 51). In this model of persistent VEEV infection, however, long-term antigen exposure, as indicated by sustained CD69 expression, was not sufficient to induce exhaustion. A recent study that examined T cell responses to chronic mouse hepatitis virus infection of the CNS also observed long-term maintenance of T cell function despite ongoing antigenic stimulation, suggesting that some aspect of the CNS regulatory environment might prevent the development of the exhaustion phenotype observed in other systems (61).

Another notable aspect of the T cell response that we observed during the subclinical chronic phase of the infection was a shift in $CD8^+/CD4^+$ T cell ratios. While this ratio was roughly 1:1 during the acute phase of the response within the CNS, by day 20 postinfection it had risen to about 3:1 and by day 70 had reached nearly 10:1. One possible explanation for this finding could be increased susceptibility to apoptosis among cells of the $CD4^+$ population. Studies performed in the context of acute lymphocytic choriomeningitis (LCMV) infection showed that $CD4^+$ memory cells have lower levels of Bcl-2 expression than $CD8^+$ memory cells and that this corresponds to a decline of greater rapidity in $CD4^+$ T cell numbers over time (24). Another possible explanation is that MHC class I and MHC class II expression within the CNS might be differentially regulated during the development of viral persistence (39). Since viral antigen presentation is likely to be required for maintenance of T cell populations during chronic infection, it may be that a reduction in MHC class II-restricted presentation could result in the gradually diminishing $CD4^+$ T cell numbers that we observed (50). More work is needed to describe the dynamics of antigen presentation within the CNS during chronic viral infection.

It has been firmly established that the CNS represents an especially unique microenvironment in which extremely tight regulation of host immune responses is essential for continued host viability (9, 37). Numerous mechanisms, including restricted expression of MHC class I and class II by neurons and the constitutive production of transforming growth factor beta (TGF-β) and immune-suppressive gangliosides by glial cells, act to limit both the magnitude and duration of inflammatory responses, thereby protecting against excessive immune pathology (15, 25, 30, 37, 48). The complex regulatory environment within the CNS might explain our observation that $CD4^+$ T cells appear to have been providing the majority of T cell-associated antiviral activity in our system. Despite both T cell populations having been clearly primed to produce IFN-γ, as evidenced by the response to PMA-ionomycin treatment, the absence of detectable IFN-γ expression by unstimulated brain-infiltrating $CD8^+$ T cells during the acute response to V3533 suggests that $CD4^+$ and $CD8^+$ cells are subject to differential regulation within the brain. This observation could be explained by a failure of infected neurons to upregulate MHC class I, preventing antigen encounter, but this is unlikely, as the vast majority of $CD8^+$ T cells retain a $CD69^+$ phenotype during both the acute and chronic phases of the response to V3533, indicating a recent encounter with cognate antigen. It seems more likely that some environmental factor is specifically limiting IFN-γ production by $CD8^+$ cells within the brain. There is precedent for this, as CNS-infiltrating $CD4^+$ T cells responding to Sindbis virus infection appear deficient in IL-2 expression, compared with $CD4^+$ T cells in the periphery (26). Other studies have shown that T cells primed by brain-resident microglia take on a phenotype that is distinct from that seen with T cells primed by other antigen-presenting cell populations (16). Clearly, further work is needed to better define the regulatory elements within the CNS that dictate T cell function during VEEV infection.

Our observation that, within this highly reductionist model, $CD4^+$ cells played a significantly more potent antiviral role than $CD8^+$ cells in response to V3533 correlated with substantially higher levels of IFN-γ expression and signs of recent degranulation. This differs from results obtained in studies performed with Sindbis virus-infected mice, where $CD4^+$ and $CD8^+$ T cells appeared to have had equivalent effects on viral titers within the CNS (5). Based on our CD8 depletion studies of μMT mice, $CD4^+$ T cells appear to exert a considerable antiviral effect, independent of any role in helping B cell or $CD8^+$ T cell responses. This effect is most likely mediated primarily by IFN-γ signaling within infected neurons, in similarity to what has been described in Sindbis virus, Borna virus, TMEV, and measles virus studies (7, 23, 38, 42). However, we cannot rule out additional mechanisms. One possible alternative mechanism could involve the release of lytic granules as $CD4^+$ T cells and, to a lesser extent, $CD8^+$ T cells both exhibited signs of recent degranulation during and after the acute-phase response. Lytic granule release could act to clear V3533 from infected neurons either by cytotoxic mechanisms (i.e., perforin release), as has been described to occur during West Nile virus infection, or by nonlethal mechanisms, as has been described to occur during HSV-1 infection (31, 52). A second possible alternative mechanism is that $CD4^+$ T cells, possibly through IFN-γ expression, might act to enhance monocyte-microglia responses to the virus, as has been observed following LCMV infection of the CNS (33). Obviously, these different mechanisms are not mutually exclusive. Given that neurons do not express MHC class II, the mechanism by which $CD4^+$ T cells recognize V3533-infected neurons also remains unclear (41).

In summary, our results confirm the importance of antiviral antibodies in limiting disease following neuronotropic alphavirus infection but also clearly demonstrate that T cells can facilitate recovery from severe viral encephalomyelitis in the absence of antibodies. The recovery that we observed in V3533-infected μMT mice was associated with a dramatic reduction in viral titers within the CNS, followed by the establishment of a persistent subclinical infection. These results demonstrate for the first time that T cells are able to directly control infection by a neuronotropic virus that causes encephalomyelitis in humans. We also showed that, in the context of VEEV infection, the majority of T cell-associated antiviral activity resides within the $CD4^+$ population, possibly due to significantly enhanced IFN-γ expression in these cells com-

pared with $CD8^+$ cells. Taken together, these findings suggest that the promotion of T cell effector function, within both $CD4^+$ and $CD8^+$ populations, should be an important consideration when designing and evaluating new vaccines against encephalitic alphaviruses.

ACKNOWLEDGMENTS

The research was supported by NIH research grant P01-AI059443. C.B.B. was supported by NIH training grant 5T32AI007419.

We thank members of the Carolina Vaccine Institute for helpful discussions. We also thank Nancy Davis, Jeff Frelinger, and Alexandra Schäfer for critical reading of the manuscript.

REFERENCES

1. **Aronson, J. F., F. B. Grieder, N. L. Davis, P. C. Charles, T. Knott, K. Brown, and R. E. Johnston.** 2000. A single-site mutant and revertants arising in vivo define early steps in the pathogenesis of Venezuelan equine encephalitis virus. Virology **270:**111–123.
2. **Bergmann, C. C., C. Ramakrishna, M. Kornacki, and S. A. Stohlman.** 2001. Impaired T cell immunity in B cell-deficient mice following viral central nervous system infection. J. Immunol. **167:**1575–1583.
3. **Bernard, K. A., W. B. Klimstra, and R. E. Johnston.** 2000. Mutations in the E2 glycoprotein of Venezuelan equine encephalitis virus confer heparan sulfate interaction, low morbidity, and rapid clearance from blood of mice. Virology **276:**93–103.
4. **Bilzer, T., and L. Stitz.** 1994. Immune-mediated brain atrophy. CD8+ T cells contribute to tissue destruction during borna disease. J. Immunol. **153:**818–823.
5. **Binder, G. K., and D. E. Griffin.** 2001. Interferon-gamma-mediated site-specific clearance of alphavirus from CNS neurons. Science **293:**303–306.
6. **Brooks, D. G., L. Teyton, M. B. Oldstone, and D. B. McGavern.** 2005. Intrinsic functional dysregulation of CD4 T cells occurs rapidly following persistent viral infection. J. Virol. **79:**10514–10527.
7. **Burdeinick-Kerr, R., and D. E. Griffin.** 2005. Gamma interferon-dependent, noncytolytic clearance of sindbis virus infection from neurons in vitro. J. Virol. **79:**5374–5385.
8. **Burdeinick-Kerr, R., J. Wind, and D. E. Griffin.** 2007. Synergistic roles of antibody and interferon in noncytolytic clearance of Sindbis virus from different regions of the central nervous system. J. Virol. **81:**5628–5636.
9. **Carson, M. J., J. M. Doose, B. Melchior, C. D. Schmid, and C. C. Ploix.** 2006. CNS immune privilege: hiding in plain sight. Immunol. Rev. **213:**48–65.
10. **Charles, P. C., J. Trgovcich, N. L. Davis, and R. E. Johnston.** 2001. Immunopathogenesis and immune modulation of Venezuelan equine encephalitis virus-induced disease in the mouse. Virology **284:**190–202.
11. **Charles, P. C., E. Walters, F. Margolis, and R. E. Johnston.** 1995. Mechanism of neuroinvasion of Venezuelan equine encephalitis virus in the mouse. Virology **208:**662–671.
12. **Davis, N. L., K. W. Brown, G. F. Greenwald, A. J. Zajac, V. L. Zacny, J. F. Smith, and R. E. Johnston.** 1995. Attenuated mutants of Venezuelan equine encephalitis virus containing lethal mutations in the PE2 cleavage signal combined with a second-site suppressor mutation in E1. Virology **212:**102–110.
13. **Davis, N. L., N. Powell, G. F. Greenwald, L. V. Willis, B. J. Johnson, J. F. Smith, and R. E. Johnston.** 1991. Attenuating mutations in the E2 glycoprotein gene of Venezuelan equine encephalitis virus: construction of single and multiple mutants in a full-length cDNA clone. Virology **183:**20–31.
14. **Diamond, M. S., E. M. Sitati, L. D. Friend, S. Higgs, B. Shrestha, and M. Engle.** 2003. A critical role for induced IgM in the protection against West Nile virus infection. J. Exp. Med. **198:**1853–1862.
15. **Fabry, Z., D. J. Topham, D. Fee, J. Herlein, J. A. Carlino, M. N. Hart, and S. Sriram.** 1995. TGF-beta 2 decreases migration of lymphocytes in vitro and homing of cells into the central nervous system in vivo. J. Immunol. **155:**325–332.
16. **Ford, A. L., E. Foulcher, F. A. Lemckert, and J. D. Sedgwick.** 1996. Microglia induce CD4 T lymphocyte final effector function and death. J. Exp. Med. **184:**1737–1745.
17. **Getts, D. R., R. L. Terry, M. T. Getts, M. Muller, S. Rana, B. Shrestha, J. Radford, N. Van Rooijen, I. L. Campbell, and N. J. King.** 2008. Ly6c+ "inflammatory monocytes" are microglial precursors recruited in a pathogenic manner in West Nile virus encephalitis. J. Exp. Med. **205:**2319–2337.
18. **Gleiser, C. A., W. S. Gochenour, Jr., T. O. Berge, and W. D. Tigertt.** 1962. The comparative pathology of experimental Venezuelan equine encephalomyelitis infection in different animal hosts. J. Infect. Dis. **110:**80–97.
19. **Grieder, F. B., N. L. Davis, J. F. Aronson, P. C. Charles, D. C. Sellon, K. Suzuki, and R. E. Johnston.** 1995. Specific restrictions in the progression of Venezuelan equine encephalitis virus-induced disease resulting from single amino acid changes in the glycoproteins. Virology **206:**994–1006.
20. **Griffin, D. E.** 2001. Alphaviruses, p. 917–962. *In* B. N. F. D. M. Knipe and P. M. Howley (ed.), Fields virology, 4th ed. Lippincott Williams & Wilkins, Philadelphia, PA.
21. **Griffin, D. E.** 2003. Immune responses to RNA-virus infections of the CNS. Nat. Rev. Immunol. **3:**493–502.
22. **Griffin, D. E., B. Levine, W. R. Tyor, P. C. Tucker, and J. M. Hardwick.** 1994. Age-dependent susceptibility to fatal encephalitis: alphavirus infection of neurons. Arch. Virol. **9**(Suppl.)**:**31–39.
23. **Hausmann, J., A. Pagenstecher, K. Baur, K. Richter, H. J. Rziha, and P. Staeheli.** 2005. CD8 T cells require gamma interferon to clear Borna disease virus from the brain and prevent immune system-mediated neuronal damage. J. Virol. **79:**13509–13518.
24. **Homann, D., L. Teyton, and M. B. Oldstone.** 2001. Differential regulation of antiviral T-cell immunity results in stable CD8+ but declining CD4+ T-cell memory. Nat. Med. **7:**913–919.
25. **Irani, D. N., K. I. Lin, and D. E. Griffin.** 1996. Brain-derived gangliosides regulate the cytokine production and proliferation of activated T cells. J. Immunol. **157:**4333–4340.
26. **Irani, D. N., K. I. Lin, and D. E. Griffin.** 1997. Regulation of brain-derived T cells during acute central nervous system inflammation. J. Immunol. **158:**2318–2326.
27. **Jackson, A. C., and J. P. Rossiter.** 1997. Apoptotic cell death is an important cause of neuronal injury in experimental Venezuelan equine encephalitis virus infection of mice. Acta Neuropathol. **93:**349–353.
28. **Jones, L. D., A. M. Bennett, S. R. Moss, E. A. Gould, and R. J. Phillpotts.** 2003. Cytotoxic T-cell activity is not detectable in Venezuelan equine encephalitis virus-infected mice. Virus Res. **91:**255–259.
29. **Juedes, A. E., and N. H. Ruddle.** 2001. Resident and infiltrating central nervous system APCs regulate the emergence and resolution of experimental autoimmune encephalomyelitis. J. Immunol. **166:**5168–5175.
30. **Kimura, T., and D. E. Griffin.** 2000. The role of CD8(+) T cells and major histocompatibility complex class I expression in the central nervous system of mice infected with neurovirulent Sindbis virus. J. Virol. **74:**6117–6125.
31. **Knickelbein, J. E., K. M. Khanna, M. B. Yee, C. J. Baty, P. R. Kinchington, and R. L. Hendricks.** 2008. Noncytotoxic lytic granule-mediated CD8+ T cell inhibition of HSV-1 reactivation from neuronal latency. Science **322:**268–271.
32. **Levine, B., J. M. Hardwick, B. D. Trapp, T. O. Crawford, R. C. Bollinger, and D. E. Griffin.** 1991. Antibody-mediated clearance of alphavirus infection from neurons. Science **254:**856–860.
33. **Lin, A. A., P. K. Tripathi, A. Sholl, M. B. Jordan, and D. A. Hildeman.** 2009. Gamma interferon signaling in macrophage lineage cells regulates central nervous system inflammation and chemokine production. J. Virol. **83:**8604–8615.
34. **Lledo, P. M., M. Alonso, and M. S. Grubb.** 2006. Adult neurogenesis and functional plasticity in neuronal circuits. Nat. Rev. Neurosci. **7:**179–193.
35. **MacDonald, G. H., and R. E. Johnston.** 2000. Role of dendritic cell targeting in Venezuelan equine encephalitis virus pathogenesis. J. Virol. **74:**914–922.
36. **Mueller, S. N., and R. Ahmed.** 2009. High antigen levels are the cause of T cell exhaustion during chronic viral infection. Proc. Natl. Acad. Sci. U. S. A. **106:**8623–8628.
37. **Niederkorn, J. Y.** 2006. See no evil, hear no evil, do no evil: the lessons of immune privilege. Nat. Immunol. **7:**354–359.
38. **Patterson, C. E., D. M. Lawrence, L. A. Echols, and G. F. Rall.** 2002. Immune-mediated protection from measles virus-induced central nervous system disease is noncytolytic and gamma interferon dependent. J. Virol. **76:**4497–4506.
39. **Pereira, R. A., D. C. Tscharke, and A. Simmons.** 1994. Upregulation of class I major histocompatibility complex gene expression in primary sensory neurons, satellite cells, and Schwann cells of mice in response to acute but not latent herpes simplex virus infection in vivo. J. Exp. Med. **180:**841–850.
40. **Perry, V. H., C. Cunningham, and C. Holmes.** 2007. Systemic infections and inflammation affect chronic neurodegeneration. Nat. Rev. Immunol. **7:**161–167.
41. **Redwine, J. M., M. J. Buchmeier, and C. F. Evans.** 2001. In vivo expression of major histocompatibility complex molecules on oligodendrocytes and neurons during viral infection. Am. J. Pathol. **159:**1219–1224.
42. **Rodriguez, M., L. J. Zoecklein, C. L. Howe, K. D. Pavelko, J. D. Gamez, S. Nakane, and L. M. Papke.** 2003. Gamma interferon is critical for neuronal viral clearance and protection in a susceptible mouse strain following early intracranial Theiler's murine encephalomyelitis virus infection. J. Virol. **77:**12252–12265.
43. **Rosenbloom, M., J. B. Leikin, S. N. Vogel, and Z. A. Chaudry.** 2002. Biological and chemical agents: a brief synopsis. Am. J. Ther. **9:**5–14.
44. **Rowell, J. F., and D. E. Griffin.** 2002. Contribution of T cells to mortality in neurovirulent Sindbis virus encephalomyelitis. J. Neuroimmunol. **127:**106–114.
45. **Ryman, K. D., W. B. Klimstra, K. B. Nguyen, C. A. Biron, and R. E. Johnston.** 2000. Alpha/beta interferon protects adult mice from fatal Sindbis virus infection and is an important determinant of cell and tissue tropism. J. Virol. **74:**3366–3378.
46. **Samuel, M. A., and M. S. Diamond.** 2005. Alpha/beta interferon protects

against lethal West Nile virus infection by restricting cellular tropism and enhancing neuronal survival. J. Virol. **79:**13350–13361.
47. **Sancho, D., M. Gomez, and F. Sanchez-Madrid.** 2005. CD69 is an immunoregulatory molecule induced following activation. Trends Immunol. **26:**136–140.
48. **Sedgwick, J. D., A. L. Ford, E. Foulcher, and R. Airriess.** 1998. Central nervous system microglial cell activation and proliferation follows direct interaction with tissue-infiltrating T cell blasts. J. Immunol. **160:**5320–5330.
49. **Sedgwick, J. D., S. Schwender, H. Imrich, R. Dorries, G. W. Butcher, and V. ter Meulen.** 1991. Isolation and direct characterization of resident microglial cells from the normal and inflamed central nervous system. Proc. Natl. Acad. Sci. U. S. A. **88:**7438–7442.
50. **Shin, H., S. D. Blackburn, J. N. Blattman, and E. J. Wherry.** 2007. Viral antigen and extensive division maintain virus-specific CD8 T cells during chronic infection. J. Exp. Med. **204:**941–949.
51. **Shin, H., and E. J. Wherry.** 2007. CD8 T cell dysfunction during chronic viral infection. Curr. Opin. Immunol. **19:**408–415.
52. **Shrestha, B., M. A. Samuel, and M. S. Diamond.** 2006. CD8+ T cells require perforin to clear West Nile virus from infected neurons. J. Virol. **80:**119–129.
53. **Simpson, D. A., N. L. Davis, S. C. Lin, D. Russell, and R. E. Johnston.** 1996. Complete nucleotide sequence and full-length cDNA clone of S.A.AR86 a South African alphavirus related to Sindbis. Virology **222:**464–469.
54. **Sitati, E. M., and M. S. Diamond.** 2006. CD4+ T-cell responses are required for clearance of West Nile virus from the central nervous system. J. Virol. **80:**12060–12069.
55. **Town, T., V. Nikolic, and J. Tan.** 2005. The microglial "activation" continuum: from innate to adaptive responses. J. Neuroinflammation **2:**24.
56. **Wang, E., R. A. Bowen, G. Medina, A. M. Powers, W. Kang, L. M. Chandler, R. E. Shope, and S. C. Weaver.** 2001. Virulence and viremia characteristics of 1992 epizootic subtype IC Venezuelan equine encephalitis viruses and closely related enzootic subtype ID strains. Am. J. Trop. Med. Hyg. **65:**64–69.
57. **Weaver, S. C., and A. D. Barrett.** 2004. Transmission cycles, host range, evolution and emergence of arboviral disease. Nat. Rev. Microbiol. **2:**789–801.
58. **Weaver, S. C., C. Ferro, R. Barrera, J. Boshell, and J. C. Navarro.** 2004. Venezuelan equine encephalitis. Annu. Rev. Entomol. **49:**141–174.
59. **Weaver, S. C., R. Salas, R. Rico-Hesse, G. V. Ludwig, M. S. Oberste, J. Boshell, and R. B. Tesh.** 1996.emergence of epidemic Venezuelan equine encephalomyelitis in South America. VEE Study Group. Lancet **348:**436–440.
60. **White, L. J., J. G. Wang, N. L. Davis, and R. E. Johnston.** 2001. Role of alpha/beta interferon in Venezuelan equine encephalitis virus pathogenesis: effect of an attenuating mutation in the 5′ untranslated region. J. Virol. **75:**3706–3718.
61. **Zhao, J., and S. Perlman.** 2009. De novo recruitment of antigen-experienced and naive T cells contributes to the long-term maintenance of antiviral T cell populations in the persistently infected central nervous system. J. Immunol. **183:**5163–5170.